

Bipartite Rokhsar–Kivelson points and Cantor deconfinementEduardo Fradkin,¹ David A. Huse,² R. Moessner,^{3,*} V. Oganesyan,² and S. L. Sondhi²¹*Department of Physics, University of Illinois at Urbana-Champaign, Urbana, Illinois 61801, USA*²*Department of Physics, Princeton University, Princeton, New Jersey 08544, USA*³*Laboratoire de Physique Théorique de l'Ecole Normale Supérieure, CNRS-UMR8549, Paris, France*

(Received 14 November 2003; revised manuscript received 12 April 2004; published 30 June 2004)

Quantum dimer models on bipartite lattices exhibit Rokhsar–Kivelson points with exactly known critical ground states and deconfined spinons. We examine generic, weak perturbations around these points. In $d=2+1$ we find a first-order transition between a “plaquette” valence bond crystal and a region with a devil’s staircase of commensurate and incommensurate valence bond crystals. In the part of the phase diagram where the staircase is incomplete, the incommensurate states exhibit a gapless photon and deconfined spinons on a set of finite measure, almost but not quite a deconfined phase in a compact $U(1)$ gauge theory in $d=2+1$! In $d=3+1$, we find a continuous transition between the $U(1)$ resonating valence bond phase and a deconfined staggered valence bond crystal. In an appendix, we comment on analogous phenomena in quantum vertex models, most notably the existence of a continuous transition on the triangular lattice in $d=2+1$.

DOI: 10.1103/PhysRevB.69.224415

PACS number(s): 75.10.Jm, 05.70.Fh, 05.50.+q, 74.20.Mn

I. INTRODUCTION

Quantum dimer models (QDMs) were introduced by Rokhsar and Kivelson¹ to capture the low-energy dynamics of valence-bond-dominated phases of quantum Heisenberg antiferromagnets.² Work on these models has established that their behavior on bipartite and nonbipartite lattices is fundamentally different. On non-bipartite lattices, they admit resonating valence bond (RVB) phases with liquid dimer correlations and deconfined (test) spinons^{3–5} that have topological order of the Z_2/BF variety.⁶ By contrast, on bipartite lattices they admit only crystalline phases^{1,7–12} [valence bond crystals (VBCs)] in $d=2$, while supporting RVB phases of the $U(1)$ or Coulomb variety in $d>2$.^{13–15}

One of the elegant features of the class of QDMs introduced in Ref. 1 is the existence of special points, christened Rokhsar–Kivelson (RK) points, at which the exact ground state wave functions are trivially determined and take the form of equal amplitude superpositions over sets of states connected by the dynamics: the classic RVB form. Additionally, test monomers have a vanishing interaction at these points, which translates into the deconfinement of gapped spinons in RVB language.³ The appropriate phase diagram for the square lattice case is sketched in Fig. 1.

In this paper, we study QDMs “near” the RK points on bipartite lattices; that is, QDMs that consist of the RK point Hamiltonians plus small, but generic, perturbations. The restriction to bipartite lattices brings an important simplification. In a sense that we will make precise below, bipartite RK points are described by gapless Gaussian field theories, and this will greatly simplify the task of analyzing perturbations.

Our basic new results are twofold. First, we establish the degree of criticality of the RK points—more precisely of the associated Gaussian field theories that are fixed points of the obvious renormalization group and to which we shall refer for clarity as the RK fixed points (RKFPs). In $d=2+1$, we show that on the honeycomb and square lattices, the RKFPs describe multicritical points with two relevant symmetric op-

erators. In $d=3+1$, the cubic lattice RKFP describes a critical point with just one relevant symmetric operator. Second, we show that the purely “staggered” phase that borders the RK points in the simplest QDMs can be pushed a finite distance away in the perturbed models and that, for $d=2+1$, the intermediate region is filled in by a devil’s staircase of commensurate and incommensurate VBCs that exhibit staggered order but also additional Bragg peaks. The commensurate crystals are gapped and confining. The incommensurate crystals exhibit a gapless photon (phason) and are deconfining, for sufficiently weak perturbations. Further, although they occur at (boundary) points, they form a generalized Cantor set of finite measure in the same limit. We refer to this phenomenon, which comes remarkably close to a deconfined phase in a compact $U(1)$ gauge theory in $d=2+1$, as Cantor deconfinement. In fact, near the RK point, this region is practically a deconfined phase, as the commensurate confined phases occupy an asymptotically small fraction of the phase diagram in this limit. In addition, the gap in the confined phases is extremely small. The possibility of such phases was pointed out previously by Levitov¹⁰ based on a mapping to the roughening problem.

This paper is organized as follows. In Sec. II, we discuss the height action for a $2+1$ -dimensional (generalized) QDMs on the square and honeycomb lattices. In Sec. III, we discuss in detail the case of the honeycomb lattice and the mechanism that drives the quantum phase transition first order in that case. In Sec. IV, we discuss the development of the tilted phase, and in Sec. V, we show that due to the strong coupling nature of these generalized dimer models, their tilted incommensurate phases generically exhibit a fully developed devil’s staircase analogous to the one discussed in two-dimensional (2D) classical systems. In Sec. VI, we discuss the phase diagram for the case of the square lattice, and in Sec. VIII, we discuss the violation of the Landau rules in these quantum phase transitions, and the deconfining nature of these quantum critical points, including the relationship of RK points to the “deconfined critical points” discussed re-

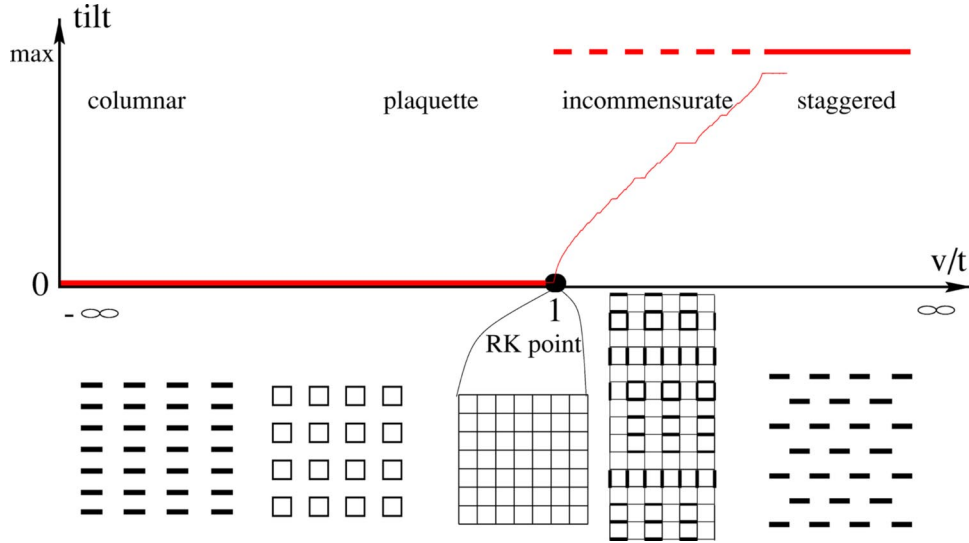


FIG. 1. Phase diagram of the square lattice QDM. In the top part of the figure, the mean tilt of the height surface is plotted as a function of v/t (see Sec. II). The corresponding dimer phases are sketched on the bottom part. The flat side (columnar and plaquette solids) terminate in the RK critical point ($v/t=1$), which has no dimer long-range order. Here, for the RK QDM (dashed line), the tilt jumps discontinuously, corresponding to a first-order transition into the staggered solid. Upon inclusion of longer-ranged interactions, however, the tilt will ascend a devil's staircase from the flat region, through a succession of incommensurate and commensurate phases. This phenomenon (and the resulting structure factor) are discussed in detail in the text.

cently by Senthil and collaborators.¹⁶ We summarize our conclusions in Sec. IX. In the Appendix, we provide a brief discussion of analogous phenomena in quantum vertex models. Here, we find that the RKFP in $d=2+1$ that controls the transition between a crystalline state and a Cantor deconfined region is critical (rather than multicritical).

II. HEIGHT ACTION IN $d=2+1$ DIMENSIONS

The Hamiltonian of the simplest quantum dimer model introduced in Ref. 1 has the form

$$\begin{aligned}
 H &= -t \left(|\bar{\square}\rangle\langle \bar{\square}| + h.c. \right) + v \left(|\bar{\square}\rangle\langle \bar{\square}| + |\bar{\square}\rangle\langle \bar{\square}| \right), \\
 H &= -t \left(|\bar{\nabla}\rangle\langle \bar{\nabla}| + h.c. \right) + v \left(|\bar{\nabla}\rangle\langle \bar{\nabla}| + |\bar{\nabla}\rangle\langle \bar{\nabla}| \right), \quad (2.1)
 \end{aligned}$$

for the square and honeycomb lattices, respectively. Here, a sum over all plaquettes of the lattice is implicit. On the honeycomb lattice,^{12,17} and with less confidence on the square lattice,^{1,7-11} it is known that the model exhibits three phases.

For $v \ll t$, it is in a “columnar” crystal phase which gives way by a first-order transition to a “plaquette” phase as v/t is increased. The plaquette phase is characterized by an order parameter that vanishes continuously at $v=t$, the RK point. At the RK point, there are multiple ground states; the exact ground state wave functions are the equal-amplitude superpositions of states in each sector of dimer configurations connected by the (off-diagonal) resonance term in Eq. (2.1). It is generally assumed that these sectors are defined by two winding numbers (see Ref. 18 for details), although a proof of ergodicity within sectors exists only for the zero winding sector.¹⁹ For $v > t$, the system enters a staggered phase in which the ground states contain no flippable plaquettes. Car-

toons of these three phases—columnar, plaquette and staggered—for the square and honeycomb lattices can be found in Figs. 1 of Refs. 11 and 12, respectively. The square case is reproduced in Fig. 1.

On bipartite lattices, the hardcore dimer constraint can be converted into a Gauss law, $\nabla \cdot \mathbf{E} = 0$. This is accomplished by endowing the links of the lattice with an orientation, so that they point from one sublattice to the other. Identifying an empty link with an electric flux -1 , and a link occupied by a dimer with a flux $z-1$ (where z is the coordination of the lattice), one obtains a lattice electric field \mathbf{E} with the desired property. In $d=2+1$, this can be solved by writing $\mathbf{E} = \nabla \times \mathbf{h}$ in terms of a scalar height field h .^{20,21} Here, the violation of the hardcore dimer covering constraint, through the presence of a monomer or overlapping dimers, shows up as a vortex in the height field.

In terms of h , the properties of the above QDMs in the vicinity of their RK points are reproduced by the imaginary time Lagrangian

$$\mathcal{L} = \frac{1}{2}(\partial_\tau h)^2 + \frac{1}{2}\rho_2(\nabla h)^2 + \frac{1}{2}\rho_4(\nabla^2 h)^2 + \lambda \cos(2\pi h), \quad (2.2)$$

with $-\rho_2 \propto (v/t) - 1$ changing sign precisely at the RK points. The last term keeps track of the discreteness of the microscopic heights, as is usual in height representations of problems in $d=2$, and we will have more to say on that later. The square and honeycomb lattice problems differ in the relevant values of ρ_4 , which are $(\pi/32)^2$ (square lattice) and $(\pi/18)^2$ (honeycomb).

To determine the operator content of these theories, one also needs to specify the compactification radius of the height variables. This is determined by the minimal uniform shift of the heights that leads to an identical dimer configu-

ration. For the cases of the honeycomb and square lattices, the compactification radii equal 3 and 4, respectively.

Finally, the details of the lattice structure enter in the relationship between lattice quantities and operators in the field theory. Specifically, long-wavelength correlations of the dimer densities n_i (where i labels the dimer direction) on the honeycomb lattice can be reconstructed by means of the leading operator identifications, given by

$$\begin{aligned} n_1 - \frac{1}{3} &= \frac{1}{3} \partial_x h + \frac{1}{2} [\exp(2\pi i h/3) \exp(4\pi i x/3) + \text{h.c.}], \\ n_2 - \frac{1}{3} &= \frac{1}{3} \left(-\frac{1}{2} \partial_x + \frac{\sqrt{3}}{2} \partial_y \right) h + \frac{1}{2} [\exp(2\pi i h/3) \exp(4\pi i x/3 \\ &\quad + 4\pi i/3) + \text{h.c.}], \\ n_3 - \frac{1}{3} &= \frac{1}{3} \left(-\frac{1}{2} \partial_x - \frac{\sqrt{3}}{2} \partial_y \right) h + \frac{1}{2} [\exp(2\pi i h/3) \exp(4\pi i x/3 \\ &\quad - 4\pi i/3) + \text{h.c.}]. \end{aligned} \quad (2.3)$$

In these expressions, x and y denote Cartesian coordinates, the x axis being perpendicular to one dimer direction. The unit of length is given by the separation of two neighboring parallel dimers. The corresponding expressions on the square lattice are

$$\begin{aligned} n_x - \frac{1}{4} &= \frac{1}{4} (-1)^{x+y} \partial_y h + \frac{1}{2} [(-1)^x \exp(\pi i h/2) + \text{h.c.}], \\ n_y - \frac{1}{4} &= \frac{1}{4} (-1)^{x+y+1} \partial_x h + \frac{1}{2} [(-1)^y \exp(\pi i h/2 + \pi i/2) + \text{h.c.}]. \end{aligned} \quad (2.4)$$

The effective Lagrangian of Eq. (2.2) was also considered in Ref. 22 in the context of the theory of classical Lifshitz (multi) critical points in three dimensions and, for this reason, this effective theory has been dubbed the quantum Lifshitz model in Ref. 23. This effective Lagrangian exhibits a three-dimensional (3D) analog of the physics of 2D classical critical isotropic systems. Thus, the action defined by Eq. (2.2) exhibits a line of fixed points parametrized by ρ_4 with $\rho_2=0$ and $\lambda=0$, under the natural momentum and frequency shell renormalization group with $z=2$. The RK points on both lattices flow under this renormalization group, to RKFPs on this line with the above values of ρ_4 . This accounts for their critical correlations and a mode spectrum $\omega \sim k^2$. In the $U(1)$ gauge theoretic interpretation of the dimer model, this mode is a photon with an anomalously soft dispersion. The irrelevance of the cosine is the necessary vanishing of the instanton effects that otherwise gap the spectrum of such compact confining theories;²⁴ this also accounts for the deconfined spinons. The height action further accounts for two other nontrivial features of the RK points; namely, that they have degenerate ground states in all winding number sectors (the RKFP point action is insensitive to gradients of heights) and that for the zero-winding states the equal time height correlations are logarithmic,

$$\langle h(\mathbf{x}, \tau) h(\mathbf{0}, \tau) \rangle = -\frac{1}{4\pi\sqrt{\rho_4}} \ln(\pi|\mathbf{x}|/a), \quad (2.5)$$

and are precisely those of the classical dimer problem. This in turn allows us to fix the values of ρ_4 quoted earlier as the classical dimer problem is exactly solvable. (This also clarifies that these values are really the fixed point values.)

On both lattices, the action [Eq. (2.2)] accounts for the plaquette crystals for $v < t$ as flat states of the height variable with different local fluctuations: when $\rho_2 > 0$, λ is relevant; that is, it is dangerously irrelevant at the RKFPs. The selection of plaquette states indicates that $\lambda < 0$ for $v/t \lesssim 1$ on both lattices. For $v > t$, $\rho_2 < 0$ the height tilts, and in the absence of any restoring term in Eq. (2.2), it attains its maximum tilt consistent with the microscopic constraints. This tilted phase translates into staggered dimer correlations which break translational symmetry on the square lattice and only rotational symmetry on the honeycomb.

The transition between the plaquette and staggered phases is somewhat unusual. As ρ_2 goes smoothly through zero at the RK point, the plaquette order vanishes *continuously* there. Further, as $v \rightarrow t^-$, there are two divergent length scales: $\chi \sim |v/t - 1|^{-1/2}$ and $\chi_c \sim (1/\sqrt{\lambda}) \chi^\theta$, with $\theta=6$, $\frac{5}{2}$ on the square and honeycomb lattices, respectively. The latter arises from the dangerously irrelevant cosine and is the length scale on which the plaquette order appears; the value of θ follows from the dimension of the irrelevant cosine at the fixed point. However, the staggered phase emerges at full strength immediately and the ground state energy density has a derivative discontinuity at the RK point, which indicates a first-order transition in the thermodynamic classification.

Let us comment briefly on the origins of the effective action of Eq. (2.2). The height representation for dimers was used or this problem by several workers; the recognition that it can be extended to capture the physics of the RK point is due to Henley,²⁵ and a more complete account of the properties of the RK point and the transition about it was given in Ref. 2. Henley's basic observation was that the Hamiltonian Eq. (2.1) also governs the master equation for the probability distribution of the classical dimer problems endowed with the simplest plaquette flip dynamics.²⁵ In height variables, the classical dimer problems are in the rough phase, so that it is reasonable that the dynamics is captured at long wavelengths by the Langevin equation

$$\partial_t h(\mathbf{x}) = -\frac{\delta S[h]}{\delta h(\mathbf{x})} + \zeta(\mathbf{x}, \tau), \quad (2.6)$$

where $S[h] \sim \int d^2x (\nabla h)^2$ is the coarse-grained entropy functional of the classical dimer problem. For Gaussian white-noise distributed ζ , the average over trajectories is weighted by the Lagrangian

$$\mathcal{L} = \left(\partial_t h + \frac{\delta S[h]}{\delta h(\mathbf{x})} \right)^2, \quad (2.7)$$

which, upon dropping a total time derivative, is the action governing the RK points.

This construction shows that the RK point action has higher dimension operators than one might have guessed on symmetry grounds alone. Indeed, the action (2.2) does not distinguish our two lattices with their different symmetries. As advertised, we are interested in this paper in weak, but otherwise generic perturbations of the Hamiltonians (2.1) about their RK points. Such generic perturbations of the RK point Hamiltonians will give rise to all operators allowed by symmetry, so that we will include them in the analysis, with the proviso that they enter with small couplings. A second implication of considering perturbed models will be that the values of the couplings in Eq. (2.2); in particular, the marginal coupling ρ_4 will also be somewhat different from their values quoted earlier: these differences will again be small. In the following, we will refer to this set of modifications as working near the RKFPs without further explanation.

A final comment is in order on an unusual aspect of the RKFPs. These fixed points, and indeed the entire fixed line, exhibit an enlarged symmetry in which the height field is free to tilt with any magnitude in any direction, which is then spontaneously broken by the ground states. While this appears to be nongeneric, such extra symmetries are a feature of any purely Gaussian fixed point. For instance, at and above $d=4$, the Ising transition is controlled by a Gaussian fixed point that is invariant under constant shifts of the scalar field. Much as in that case we work near zero field (magnetization), in our problem, we will work near zero tilt. In both cases, this is the correct choice for a sector of the space of couplings—the sector in which the transition is continuous in mean-field theory.

III. EXPANDED ACTION ON HONEYCOMB LATTICE

We turn now to the honeycomb lattice. For honeycomb dimers, the heights live on the triangular lattice, which naively indicates an action rotationally invariant to fourth order in gradients. However, the microscopic heights have a sublattice structure: they take values 0, 1 and 2 *modulo* 3 on the three sublattices of the triangular lattice. Consequently, the symmetries of rotation by $\pi/3$ and inversion also involve sending $h \rightarrow -h$. It follows then that the allowed nonirrelevant operators at the RKFP include the relevant cubic term

$$\mathcal{L}_3 = g_3(\partial_x h) \left(\frac{1}{2} \partial_x h - \frac{\sqrt{3}}{2} \partial_y h \right) \left(\frac{1}{2} \partial_x h + \frac{\sqrt{3}}{2} \partial_y h \right) \quad (3.1)$$

in addition to the marginal coupling

$$\mathcal{L}_4 = g_4 [\nabla h \cdot \nabla h]^2. \quad (3.2)$$

The growth of g_3 in the infrared indicates that the criticality of the RK point does not survive its inclusion; the form of the interaction indicates that when g_3 is nonzero the system has already entered the tilted phase, although with the tilt now locked to the lattice. This leads us to conclude that the transition between the flat plaquette phase and the tilted phase goes truly first order.

If we tune g_3 to zero, we can examine the stability of the multicritical RK point. In a renormalization group treatment, where we keep a cutoff in space alone, the lowest nontrivial order flows of the two interactions are

$$\frac{d\lambda}{dt} = - \left(\frac{\pi}{2\rho_4^{1/2}} - 2 \right) \lambda,$$

$$\frac{dg_4}{dt} = - \frac{9}{4\pi\rho_4^{3/2}} g_4^2, \quad (3.3)$$

whence both interactions are irrelevant for $g_4 > 0$.²² As g_4 is marginally irrelevant it produces logarithmic corrections and the flows also renormalize ρ_4 thus parking the system elsewhere on the fixed line. With these observations, we see that the multicritical behavior represented by the RK point is stable on a surface of codimension 2, provided the long-wavelength $\rho_4 \leq (\pi/4)^2$. The latter condition holds for small perturbations of Eq. (2.2).

IV. THE TILTED PHASE

Once g_4 is large enough, the tilt no longer jumps to its maximum value on leaving the flat phase. When g_3 is nonzero, the tilt prefers to point along one of the dimer directions or in between two dimer directions depending on the sign of this coupling. A similar role is played by \tilde{g}_4 on the square lattice (see below). Here, the restriction to small tilts is crucial: the states for $g_3 > 0$ and $g_3 < 0$ are *not* related by symmetry. In particular, at large tilts there are only states with one sign of the tilt; that is, with the dimers dominantly oriented along the three bond directions. We also note that on traversing the multicritical point with $g_3 = 0$, the same orientational selection is now affected by the fifth-order term

$$\mathcal{L}_5 = g_5 (\nabla h)^2 (\partial_x h) \left(\frac{1}{2} \partial_x h - \frac{\sqrt{3}}{2} \partial_y h \right) \left(\frac{1}{2} \partial_x h + \frac{\sqrt{3}}{2} \partial_y h \right), \quad (4.1)$$

which is thus dangerously irrelevant at the multicritical fixed point.

The properties of the tilted phase can be analyzed by expanding in small fluctuations about the weakly tilted state (henceforth, we assume $g_3 < 0$, so that the tilt is along the x axis, and that $|g_3|$ is small)

$$h(\mathbf{r}, \tau) = \mathbf{C} \cdot \mathbf{r} + \delta h(\mathbf{r}, \tau), \quad \mathbf{C} = \mathbf{C}\mathbf{x}. \quad (4.2)$$

The corresponding Goldstone action is given (to quadratic order in fluctuations) by

$$\delta\mathcal{L} = \frac{1}{2} (\partial_\tau \delta h)^2 + \frac{\rho_4}{2} (\nabla^2 \delta h)^2 + \frac{v_l^2}{2} (\partial_x \delta h)^2 + \frac{v_t^2}{2} (\partial_y \delta h)^2. \quad (4.3)$$

Higher order terms (in δh) are irrelevant due to nondivergence of fluctuations. Provided $|\rho_2| < g_3^2/g_4$, then $v_l \approx v_t$ and a single correlation length can be defined, $\xi^{-1} = v_l/\sqrt{\rho_4}$, so that for sufficiently large momenta, $q > \xi^{-1}$, and the spectrum is quantum critical, while as $q \rightarrow 0$, the modes acquire a stiffness, and their dispersion is linear with longitudinal and transverse velocities given by v_l and v_t , respectively. The average tilt of the height variable translates into new Bragg peaks appearing in the structure factor for the dimer densities

[as deduced from Eqs. (2.3) and (2.4)]. They are of two types: first is the *commensurate* Bragg peak at the wave vector of the maximally staggered state located at the origin for the honeycomb case [and at (π, π) in the case of the square lattice], the second type are the *incommensurate* peaks displaced from the characteristic wave vectors of the columnar/plaquette pattern [e.g., $(4\pi/3, 0)$ and $(\pi, 0)$ on honeycomb and square lattices, respectively] by an amount proportional to C . In the tilted regime, the intensity of the commensurate peak varies as C^2 , while that of the incommensurate peaks as $\xi^{-\pi^9/\rho_4}$ (on the square lattice as $\xi^{-\pi/16\rho_4}$). Generally, as a result of quantum critical fluctuations, the two peaks differ in intensity parametrically, both intensities becoming C^2 for ρ_4 corresponding to the purely short-range Hamiltonian of Eq. (2.1). The existence of gapless modes has important implications; one of them is that test monomers (spinons) interact through a potential that generally grows only logarithmically with distance, as opposed to the linearly growing *confining* potential encountered in commensurate valence bond solids.

V. INCOMMENSURATE LOCKED CRYSTAL PHASES: THE DEVIL'S STAIRCASE

The actual state of the system involves an interplay between the propensity of the system to establish a tilt discussed thus far and the discreteness of the microscopic heights. As we will quantify a little later, the operators encoding the discreteness are much more irrelevant (although dangerously so, see below) at the RKFP than those responsible for the selection of the tilt magnitude and direction. Therefore, near the RKFP, the problem can be treated in the order in which we have discussed it. Away from this limit, one can worry about more complex phase diagrams.

In order to treat height discreteness properly, we need to generalize our treatment of the discreteness of the height in Eq. (2.2). There, we included a potential that favors discrete, flat configurations of the height field, but in doing so, we ignored the possibility of the height locking into tilted configurations. To identify the full set of locking potentials, we note that the height and the lattice points together define a 3D lattice with points (h, \mathbf{x}) . A general locking potential, in particular the one generated from the microscopic constraints under renormalization, can be expanded in the set of reciprocal lattice vectors $\{\mathbf{G}\}$ of this 3D lattice, given by

$$V_{\text{lock}}(h, \mathbf{x}) = \sum_{\{\mathbf{G}\}} V_{\mathbf{G}} e^{i(G_h h + \mathbf{G}_x \cdot \mathbf{x})}, \quad (5.1)$$

and thus each \mathbf{G} defines a locking potential. Nicely enough, the height–space lattice for the honeycomb dimer problem is the simple cubic lattice with the [111] direction measuring height, so that working out the set of locking potentials is particularly simple.

As discussed in the previous section, in the tilted phase the mean-square fluctuations of the height are finite. As a consequence of this, whenever the average tilt of the height surface is commensurate with the lattice, the corresponding terms in the locking potential (above) are asymptotically relevant. At such points the ground state is a commensurate valence bond crystal with a gapped spectrum. At incommen-

surate tilts the outcome depends upon the strength of V_{lock} relative to the remaining quantum fluctuations. When the latter are strong, as is the case for small tilts, the ground state at most tilts is an incommensurate VBC with a Bragg peak at the incommensurate wave vector but with a gapless (phason) spectrum. In the gauge theoretic interpretation of the dimer model, this excitation is a photon and correspondingly test monomers are deconfined, in that they experience the logarithmic interaction of free 2D electrodynamics. If the locking potential is increased and/or the quantum fluctuations decreased, we expect a version of Aubry's "breaking of analyticity"²⁶ transition beyond which the incommensurate ground states are pinned, their low-lying excitations are localized though still gapless, and the incommensurate ground states occupy a set of measure zero in the phase diagram.

The weak locking regime exists, parametrically, at small tilts near the RK point. For concreteness, consider approaching the multicritical surface by tuning g_3 with ρ_2 set equal to zero. The closer we get to the transition, the higher order the commensuration that leads to locking, with $|\mathbf{G}| \sim 1/C$ or larger. This has various effects: first, the coefficients of the corresponding locking potentials generally decrease as one goes to larger \mathbf{G} ; second, the operators become increasingly irrelevant at the RK fixed point; and third, the length scale increases at the crossover from the quantum critical regime, in which the locking potential is irrelevant to the tilted regime, where it becomes relevant. These effects combine together to make the renormalized strength of the locking potential, and thus the size of the gap in each commensurate phase, as well as the width of the parameter range in the phase diagram occupied by the phase, all vanish at small tilts C exponentially in $1/C^2$; for example, the gap

$$\Delta \sim C^{a(\rho_4 C^2)}. \quad (5.2)$$

As the correlation length $\xi \propto 1/C$, this is equivalent to an ordering length that grows rather fantastically, as

$$\xi_c \sim \xi^{a' \xi^2/\rho_4}, \quad (5.3)$$

where a and a' are positive constants. Consequently, even the commensurate phases are for all practical purposes gapless in this weak-tilt regime. Thus, when the tilting transition is either continuous or very weakly first order, there is a deconfined, weakly ordered dimer-crystal phase near the RK point where the ordering is generically incommensurate! By contrast, the existence of the strong locking regime will need to be determined by actual solution of the relevant models; the existence of the fully tilted states is not proof of strong locking, merely of the existence of a maximum tilt as a consequence of the periodicity of the height variable.

Returning to the infinite-volume and zero-temperature phase diagram, the commensurate and incommensurate states will be interleaved in the classic manner of the devil's staircase studied in a variety of commensurate–incommensurate problems.²⁷ At weak locking, close to the RK point, the staircase is incomplete; that is, the deconfined incommensurate points will form a set of finite measure as the control parameter, ρ_2 or g_3 , is varied. In fact, the fraction of the phase diagram occupied by the incommensurate de-

confined states approaches unity as the RK point is approached. This is the phenomenon we have termed Cantor deconfinement. Farther away from the RK point, the staircase could become complete, with the incommensurate points being a set of zero measure, before the maximally tilted phase is reached. Needless to say, this scenario assumes that no first-order transitions intervene.

Finally, a brief comment on Bragg peaks. The actual details of the ordering—periodic in the commensurate states and quasiperiodic in the incommensurate states—will cause the second peak to fragment into multiple and even a dense set of higher-order Bragg peaks.

VI. EXPANDED ACTION ON THE SQUARE LATTICE

On the square lattice, the generic case requires that we (a) allow ρ_4 to vary, (b) include the quadratic and strictly marginal term

$$\mathcal{L}_m = \frac{1}{2}\tilde{\rho}_4[(\partial_x^2 h)^2 + (\partial_y^2 h)^2], \quad (6.1)$$

and (c) include the interactions

$$\mathcal{L}_{\text{int}} = g_4[\nabla h \cdot \nabla h]^2 + \tilde{g}_4[(\partial_x h)^4 + (\partial_y h)^4]^2. \quad (6.2)$$

The impact of (a) and (b) together is that we are interested in flows about a 2D surface of fixed points. Unlike the honeycomb lattice, there is no cubic invariant so that the transition is continuous at the level of mean-field theory for the height action. However, there are two tree-level marginal couplings whose fate needs to be decided by fluctuations. Let us focus for now on the flow around the fixed line with $\tilde{\rho}_4=0$.

The lowest nontrivial order flows of interest are

$$\begin{aligned} \frac{d\lambda}{dt} &= -\left(\frac{\pi}{2\rho_4^{1/2}} - 2\right)\lambda, \\ \frac{dg_4}{dt} &= -\frac{9}{4\pi(\rho_4)^{3/2}}\left(g_4^2 + g_4\tilde{g}_4 + \frac{1}{4}\tilde{g}_4^2\right), \\ \frac{d\tilde{g}_4}{dt} &= -\frac{9}{4\pi(\rho_4)^{3/2}}\left(\frac{2}{3}g_4\tilde{g}_4 + \frac{1}{2}\tilde{g}_4^2\right). \end{aligned} \quad (6.3)$$

Interestingly, the flows in the (g_4, \tilde{g}_4) plane are attracted to the origin only along the positive g_4 axis; generically, the flows run away to the region where the action is unstable at quartic order in gradients. From this we conclude that it is highly likely that the transition is driven first order by fluctuations in the generic case. Now, the RK point behavior requires a further fine tuning, $\tilde{g}_4=0$, and hence it represents the behavior of a multicritical surface of codimension two. We find that the inclusion of a small $\tilde{\rho}_4$ does not alter the topology of the flows and there remains only one trajectory flowing into the fixed point at the origin.

For the runaway flows, the pattern of symmetry breaking is indicated by the initial sign of \tilde{g}_4 , and depending on that, we find four states with the tilt either aligned or at angle $\pi/4$ to the lattice axes. All of them exhibit, necessarily, a modulation of the dimer density at wave vector (π, π) . If $\tilde{g}_4=0$, the sixth-order term is now responsible for the orientational selection.

The analysis of the tilted phase now requires identifying the reciprocal lattice vectors of the diamond lattice, with its [100] direction measuring the height. The qualitative features of the devil's staircase are exactly as in the honeycomb case. Bragg peaks now appear at (π, π) and near $(\pi, 0)$ and $(0, \pi)$.

VII. THE CUBIC LATTICE

We turn finally to the case of the $d=3$ cubic lattice. Now, the constraint is solved by introducing a gauge field \mathbf{A} , in terms of which the action is of the form¹⁴

$$\mathcal{L} = \frac{1}{2}(\partial_t \mathbf{A})^2 + \frac{1}{2}\rho_2(\nabla \times \mathbf{A})^2 + \frac{1}{2}\rho_4(\nabla \times \nabla \times \mathbf{A})^2, \quad (7.1)$$

with $\rho_2=0$ again signaling the RK point. In gauge-invariant notation, the quadratic terms become the squares of the electric and the corresponding magnetic field in $d=3+1$.

The discreteness of the microscopic fields is irrelevant in a finite interval around the RK point and hence can be ignored in its proximity. The only nonirrelevant term consistent with cubic symmetry missing from Eq. (7.1) is

$$\tilde{\rho}_4 \sum_i [\partial_i(\nabla \times \mathbf{A})_i]^2, \quad (7.2)$$

which is strictly marginal. Hence the critical behavior represented by the RK point is (marginally) stable. The additional coupling leads to rotationally noninvariant critical points.

For $\rho_2 < 0$, we need to include the (dangerously) irrelevant terms that control the magnitude of the “magnetic field,” $\mathbf{B} = \nabla \times \mathbf{A}$. These are \mathbf{B}^4 and $B_x^4 + B_y^4 + B_z^4$ and lead to staggered crystals [now with a modulation of the dimer density at (π, π, π)] aligned parallel or intermediate to the lattice axes. The connected correlations of the dimer density exhibit distorted dipolar correlations. This spectrum exhibits a gapless photon with fluctuations of the fields about their ground state values, and deconfined spinons. Altogether, one obtains critical points separating a liquid of dimers from a crystal. At larger tilts, confinement and further symmetry breaking can be expected to set in, but that is outside the validity of our analysis.

We also note that other related problems, such as the two-dimer model on the bipartite diamond lattice studied by Hermele *et al.*¹⁵ in its incarnation as a pyrochlore Ising antiferromagnet with Ising dynamics, will *mutatis mutandis* exhibit the same phase diagram.

VIII. LANDAU RULES AND ORDER PARAMETER THEORIES

In Ref. 2, three of us commented that the RK point in the simplest bipartite QDMs in $d=2+1$ sat at the transition between two symmetry incompatible VBCs and attributed the divergence of the correlation length at it to the deconfinement of the gauge/height field at the RK point. Recently, Senthil *et al.*¹⁶ have considered a similar scenario for the transition between a Néel state and a VBC although now with dynamical spinons, and christened the intervening critical point a deconfined critical point.

At issue in these discussions are two distinct but closely related possibilities. First, the violation of the Landau rule that a phase transition between two symmetry incompatible phases must generically be first order, except at multicritical points. Second, the formulation of the theory of the phase transition in terms of fields other than the order parameters of the proximate phases. At a technical level, this happens when the ordering is driven by dangerously irrelevant operators.

As we have discussed in this paper, the situation near the RK points is more complicated than was assumed in Ref. 2. Instead of a single tilting transition between the plaquette phase and the staggered phase, there is a devil's staircase of commensurate–incommensurate transitions. Nevertheless, sufficiently close to the RK point, any commensurate ordering is extremely weak, and for practical purposes one can think of the RKFPs controlling a continuous transition between a flat phase with plaquette order and a tilted phase with staggered order as well as incommensurate order with a continuously varying wave vector. The weakly tilted phase, however, is (logarithmically) deconfined, unlike the fully tilted staggered phase.

In the quantum dimer models analyzed in this paper, the RKFPs control multicritical surfaces, in contradiction with the claim in Ref. 2. However, this is not inevitable in this class of problems. A quantum vertex model discussed in the Appendix exhibits a critical surface controlled by RKFPs. In either case, the underlying height action [Eq. (2.2)] is not derived from the order parameters of the proximate phases. In this sense, they lie outside the Landau paradigm when applied to quantum phase transitions.

Finally, we note that in the $d=3+1$ cubic QDM, the tilting transition remains continuous for weakly perturbed QDMs, and that the tilted phase exhibits only staggered correlations. This is now a continuous transition inside a deconfined region where Landau theory predicts a continuous transition. That said, the critical theory is still not what one would naively deduce from an order parameter analysis of the ordered (staggered) phase: the correlations of the order parameter at criticality have a dipolar form. The complication is the need to properly treat the local constraint $\nabla \cdot \mathbf{E}=0$, which is accounted for in the action Eq. (7.1) by the introduction of the vector potential \mathbf{A} . It is also the case that the ordered phase breaks rotational symmetry due to a dangerously irrelevant operator. Altogether, while the 3D problem is not quite as unusual as the 2D one, it also furnishes an instance in which the critical theory requires a departure from the standard cookbook.

IX. SUMMARY

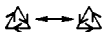
We have analyzed the phase diagram in the vicinity of the RK points in the bipartite QDMs. In $d=2$, we find a first-order transition separating confining plaquette phases from a devil's staircase of commensurate/incommensurate and confining/deconfining VBCs on both the honeycomb and square lattices with the RK points sitting on a multicritical surface of codimension 2. In $d=3$, the RKFP controls a continuous transition between an RVB phase and a deconfined

staggered VBC. QDMs that exhibit these phenomena can be constructed by adding multidimer potential energies to the RK point Hamiltonians. Whether the phenomena here can be identified in a spin model or in other physical systems, is an interesting topic for future work. Finally, we note that as we were writing up this work, there appeared Ref. 28, which has considerable overlap with our work, but which differs from our conclusions on some points.

ACKNOWLEDGMENTS

We would like to thank P. Fendley, C. Henley, J. Kondev, S. Sachdev, and T. Senthil for useful discussions; the latter especially for focusing our attention on the implications of lattice symmetries. This work was in part supported by the Ministère de la Recherche et des Nouvelles Technologies with an ACI grant (R.M.), by the National Science Foundation grants NSF-DMR-9978074 and NSF-DMR-0213706 at Princeton University (S.L.S., D.A.H., and V.O.), NSF-DMR-01-32990 at the University of Illinois (E.F.), and by the David and Lucile Packard Foundation (S.L.S. and V.O.).

APPENDIX: QUANTUM VERTEX MODELS

Quantum vertex models are close cousins of QDMs. Here, we begin with a Hilbert space labeled by configurations of a classical vertex model, that is, each bond hosts an Ising variable that we picture as an arrow marked on it. We then introduce a local quantum dynamics which consists of reversing local closed loops of arrows. In cartoon form, the resonance move analogous to the one captured in Eq. (2.1) is given by 

As the bond variables here are oriented, their physical origins will necessarily be distinct from those of dimers. For example, a quantum six-vertex model was introduced in Ref. 29 as a model for quantum effects in 2D ice as well as via a mapping from a planar pyrochlore Ising magnet placed in a transverse magnetic field. Subsequently, it has also been argued to arise as an effective theory of the quantum fluctuations in the d -density wave state where the microscopic variables are oriented currents.³⁰

An exhaustive analysis of the RK point manifold in the quantum eight-vertex model is contained in Ref. 23. When critical, the model is equivalent to the six-vertex model. In this case, the conservation law at the vertices leads straightforwardly to a height representation in which the two sublattices of the square lattice host even and odd values of a height field with circumference 2. A nice feature of the quantum six-vertex problem is that one can find a family of RK points at which the value of ρ_4 can be tuned continuously; the ground state wave functions in these cases are no longer equal-amplitude superpositions, but still exhibit isotropic critical correlations. The analysis of perturbations of these RK points now closely parallels our discussion of the square lattice QDM and we conclude that they govern a multicritical surface, likely between a plaquette phase³¹ and a devil's staircase region. The significant differences from the dimer case involve (a) the degeneracies of the phases and (b) the varying dimension of the vertex operator piece of the dimer

operator. The latter causes the relative strengths of the staggered order and incommensurate order to vary in the tilted phase. For example, near the equal-amplitude RK point, the staggered order is quadratic in the tilt as against cubic for the incommensurate piece.

Of the 32 possible vertices on a triangular lattice, 20 conserve the number of arrows and hence permit a height representation. The heights live on the dual honeycomb lattice and are even and odd on its two sublattices with circumference 2. The symmetries now force the height action to be even in h and isotropic to fourth order in gradients. Consequently, the line of RK fixed points is now stable with a dangerously irrelevant sixth-order term picking one of six lattice directions to orient the tilted phase. The (h, \mathbf{x}) lattice is an hcp structure with in-plane bonds deleted and its recip-

rocal lattice vectors govern the commensurate states in the devil's staircase region.

The values of ρ_4 stemming from particular microscopic models in this family are under investigation and will be reported more fully elsewhere;³² here, we content ourselves with noting that at the equal-amplitude RK point, the height is rough³² and hence in its neighborhood we now have an example of critical behavior governed by RK fixed points and a Cantor deconfined region which can be accessed without dialing the extra parameter needed in the dimer models discussed previously in this paper. Based on experience with this class of models, it seems likely that the flat phase is again a plaquette phase which is symmetry incompatible with the Cantor region.

*Email address: moessner@lpt.ens.fr

¹D. S. Rokhsar and S. A. Kivelson, Phys. Rev. Lett. **61**, 2376 (1988).

²See R. Moessner, S. L. Sondhi, and E. Fradkin, Phys. Rev. B **65**, 024504 (2002), for an introduction to quantum dimer models from the present perspective.

³R. Moessner and S. L. Sondhi, Phys. Rev. Lett. **86**, 1881 (2001).

⁴G. Misguich, D. Serban, and V. Pasquier, Phys. Rev. Lett. **89**, 137202 (2002).

⁵R. Moessner and S. L. Sondhi, Phys. Rev. B **68**, 054405 (2003).

⁶X.-G. Wen, Phys. Rev. B **44**, 2664 (1991); T. H. Hansson, V. Oganesyan, and S. L. Sondhi, cond-mat/0404327 (unpublished).

⁷S. Sachdev, Phys. Rev. B **40**, 5204 (1989).

⁸L. B. Ioffe and I. E. Larkin, Phys. Rev. B **40**, 6941 (1989).

⁹E. Fradkin and S. A. Kivelson, Mod. Phys. Lett. B **4**, 225 (1990).

¹⁰L. S. Levitov, Phys. Rev. Lett. **64**, 92 (1990).

¹¹P. W. Leung, K. C. Chiu, and K. J. Runge, Phys. Rev. B **54**, 12938 (1996).

¹²R. Moessner, S. L. Sondhi, and P. Chandra, Phys. Rev. B **64**, 144416 (2001).

¹³D. A. Huse, W. Krauth, R. Moessner, and S. L. Sondhi, Phys. Rev. Lett. **91**, 167004 (2003).

¹⁴R. Moessner and S. L. Sondhi, Phys. Rev. B **68**, 184512 (2003).

¹⁵M. Hermele, M. P. A. Fisher, and L. Balents, Phys. Rev. B **69**, 064404 (2004).

¹⁶T. Senthil, A. Vishwanath, L. Balents, S. Sachdev, and M. P. A. Fisher, Science **303**, 1490 (2004).

¹⁷N. Read and S. Sachdev, Nucl. Phys. B **316**, 609 (1989); Phys. Rev. Lett. **62**, 1694 (1989); Phys. Rev. B **42**, 4568 (1990).

¹⁸See E. Fradkin, *Field Theories of Condensed Matter Systems* (Addison-Wesley, Redwood City, 1991), Chap. 6, where there is a detailed discussion of the winding numbers in the quantum dimer model on the square lattice as a gauge theory, its connection with quantum roughening (or height) models, and of the deconfining character of the RK point.

¹⁹W. Thurston, Am. Math. Monthly **97**, 757 (1990).

²⁰R. Youngblood, J. D. Axe, and B. M. McCoy, Phys. Rev. B **21**, 5212 (1980).

²¹E. Fradkin and S. A. Kivelson, Mod. Phys. Lett. B **4**, 225 (1990).

²²These flows were studied previously in a different, classical, context by G. Grinstein, Phys. Rev. B **23**, 4615 (1981).

²³The $d=2$ classical to $d=3$ quantum connection is present also at the level of the wave function of the quantum model which is given by the statistical Gibbs weight of the 2D classical Gaussian model. Thus, at an RK quantum critical point, these systems have scale invariant ground state wave functions. This and other aspects of this problem are discussed in E. Ardonne, P. Fendley, and E. Fradkin, Ann. Phys. (N.Y.) **310**, 493 (2004).

²⁴A. M. Polyakov, Nucl. Phys. B **120**, 429 (1977).

²⁵C. L. Henley, J. Stat. Phys. **89**, 483 (1997); cond-mat/0311345 (unpublished).

²⁶S. Aubry, in *Solitons in Condensed Matter Physics*, edited by A. Bishop and T. Schneider (Springer, Berlin, 1978), p. 264.

²⁷P. Chaikin and T. Lubensky, *Principles of Condensed Matter Physics* (Cambridge University Press, Cambridge, 1995), Chap. 10 contains a fine introduction to this set of ideas. The important ideas on the connection between the Kolmogorov-Arnold-Moser (KAM) theorem in classical dynamics and the existence of the weak locking regime that underlie our assertions in this section are discussed in E. H. Fradkin, O. Hernandez, B. A. Huberman, and R. Pandit, Nucl. Phys. B **215**, 137 (1983).

²⁸A. Vishwanath, L. Balents, and T. Senthil, Phys. Rev. B **69**, 224416 (2004).

²⁹R. Moessner, O. Tchernyshyov, and S.L. Sondhi, J. Stat. Phys. **116**, 755 (2004).

³⁰S. Chakravarty, Phys. Rev. B **66**, 224505 (2002).

³¹See Ref. 29 and Ph. Sindzingre (unpublished).

³²S. Isakov and R. Moessner (unpublished).